PERGAMON

Solid State Communications 123 (2002) 87–92

solid state communications

www.elsevier.com/locate/ssc

Photoluminescence studies of isotopically enriched silicon: isotopic effects on the indirect electronic band gap and phonon energies

D. Karaiskaj[a,*], M.L.W. Thewalt[a], T. Ruf[b], M. Cardona[b], M. Konuma[b]

[a]*Department of Physics, Simon Fraser University, Burnaby, BC, Canada V5A 1S6*
[b]*Max-Planck-Institut für Festkörperforschung, 70569 Stuttgart, Germany*

Received 15 April 2002; received in revised form 6 June 2002; accepted 7 June 2002 by D.J. Lockwood

Abstract

We have performed high-resolution photoluminescence spectroscopy on silicon crystals with different isotopic composition and investigated the effects of this composition on the indirect electronic band gap and phonon energies. From the relative energy shift of the indirect electronic band gap between two crystals of different isotopic composition, the zero-point renormalization energy of that electronic band gap was estimated. The experimentally determined phonon frequency shifts between crystals of different isotopic composition are compared with theoretically predicted frequency shifts. We further present a detailed analysis of the different contributions leading to the observed phonon frequency shifts.

PACS: 78.55.Et; 71.35.Cc

Keywords: A. Isotopic silicon; B. Excitons bound to impurities; B. Phonons; E. Luminescence

1. Introduction

The availability of semiconductor crystals that are chemically pure and highly enriched isotopically has made it possible to study the effects of the isotopic composition on the lattice dynamics and electronic properties of these materials [1–6]. The simplest approximation, the harmonic virtual crystal approximation (VCA), predicts that the phonon energy decreases proportionally to the inverse square root of the average isotopic mass. In addition to that, isotopic disorder effects, which cause energy shifts and broadenings of the phonon modes, have to be taken into account. Previous studies have shown that the isotopic composition causes an energy shift of the electronic band gap of semiconductor materials. This energy shift is to first approximation proportional to the inverse square root of the average isotopic mass and is mainly due to the direct electron–phonon interaction and to a lesser extent to the change of the lattice constant with the isotopic mass, in the so-called quasiharmonic approximation. [1–14].

The electronic states of crystals, such as valence and conduction band states, are renormalized by their interaction with phonons [15,16]. By changing the temperature of the crystal, its electronic states shift energetically mostly due also to direct electron–phonon interaction. Crystal vibrations exist also at zero Kelvin (zero-point vibrations) and interact with electrons renormalizing their energy. Changes in the average isotopic mass lead to changes in the lattice vibrations and, as a consequence of the electron–phonon interaction, to an energy shift of the electronic states. A simple explanation for the effects of isotopic composition on the electronic band gap due to electron–phonon interaction can be given via perturbation theory and Feynman diagrams [16]. This effect can be broken up into two contributions: the Debye–Waller and the 'self-energy' terms. Both terms are obtained from a perturbative calculation of the electron self-energy to second-order in atomic displacement. The Debye–Waller correction is an effect of the second-order electron–phonon interaction

* Corresponding author.

0038-1098/02/$ - see front matter
PII: S0038-1098(02)00249-1

taken to first-order in perturbation theory and depends only on the phonon amplitude and not on the phonon involved. The self-energy contributions, which are different for each electronic state and also for each phonon involved, arise from the first-order electron–phonon interaction taken to second-order in perturbation theory. If we consider these two contributing terms, we find that the isotope effect on the one-electron states at a given temperature is proportional to the averaged squared phonon amplitude [1,8].

$$|\langle\vec{u}(\vec{Q}j)\rangle|^2 = \frac{\hbar^2}{2M_\nu N\Omega_{\vec{Q}j}}[1+2n_{\vec{Q}j}(T)] \tag{1}$$

where M_ν is the mass of one atom of type ν and $n_{\vec{Q}j}(T)$ the occupation number of the phonon with the wave vector Q, branch j, and energy $\Omega_{\vec{Q}j}$ and N is the number of unit cells. At low temperatures the occupation number (Bose–Einstein factor) can be approximated by $n_{\vec{Q}j}(T) \approx 0$ which leads to:

$$|\langle\vec{u}(\vec{Q}j)\rangle|^2 \propto 1/\sqrt{M_\nu} \tag{2}$$

Hence, isotope shifts in the electronic band gaps are observed at low temperatures. At such temperatures, the isotope effects are usually generated by the mean squared phonon amplitude through the electron–phonon interaction. They should be related to the average isotopic mass ($\bar{M}$) through:

$$\Delta E^{\text{elec}} \propto \frac{1}{\sqrt{\bar{M}}} \tag{3}$$

If two samples with different isotopic composition are available and the energy shift of the electronic band gap induced by the change in isotopic composition can be determined experimentally, the full amount of the renormalization by the zero-point vibrations can be estimated [1]. Using Eq. (3) it can be shown that,

$$\Delta E^{\text{elec}} = E^{\text{elec}}\frac{M(A)-M(B)}{M(A)+M(B)} \tag{4}$$

In Eq. (4) ΔE^{elec} represents the energy shift of the electronic band gap, E^{elec} the zero-point band gap renormalization energy, $M(A)$ and $M(B)$ the average isotopic masses of two crystals with different isotopic composition.

As mentioned earlier in this paper, the isotopic composition of the crystal also changes the energy of the lattice vibrations. In the simplest approximation, the phonon frequencies depend only on the inverse square root of the average vibrating mass (VCA),

$$\omega_1/\omega_2 = \sqrt{M_2/M_1} \tag{5}$$

In reality, additional interactions influence the phonon energies and lifetimes, such as anharmonic and disorder effects [1–3,9–14,17–24]. The anharmonic contributions to the frequency shift result from the phonon–phonon interaction and modify the phonon energies proportional to the inverse average vibrating mass. The coherent potential approximation (CPA) enables us to estimate disorder contributions to the energy shift and broadening of the phonons with isotopic composition [18]. This model takes into account a random distribution of the different isotopes that, together with phonon decays (anharmonic effects), contributes to the phonon frequency shifts and lifetimes. The disorder-induced effects, considered by the CPA, are related to the one-phonon density of states (DOS); this relationship is univocal for monatomic crystals. Recent CPA calculations using the one-phonon DOS of germanium given in Ref. [25], renormalized so as to correspond to silicon [26], have been able to explain the disorder induced shifts and broadenings for different phonons in silicon [18].

2. Experiment and discussion

In this article, we present photoluminescence (PL) data obtained from chemically pure (not intentionally doped, but containing boron (B) and phosphorus (P) impurities which are the most common shallow donor and acceptor contaminants in Si) and isotopically enriched silicon samples of different isotopic compositions. The PL spectra were collected from samples mounted in a strain-free manner and immersed in liquid He at a bath temperature of either 4.2 or 1.3 K, with excitation provided either by the 514.5 nm line of an Ar^+ laser or, in order to ensure bulk excitation, 1020 nm of a Ti-sapphire laser with line narrowing provided by an intracavity etalon for precision measurement of the Raman line. The excitation densities used were between 0.3 and 0.6 W/cm^2. The natural Si sample used for comparison was a float-zone crystal selected to have approximately the same B and P concentration as the isotopically enriched ^{28}Si crystal. The spectra were collected with a Bomem DA8 Fourier transform interferometer using a cooled Ge detector.

The isotopic composition and the estimated average masses of all crystals investigated are given in Table 1. The PL spectra of natural Si, isotopically enriched ^{28}Si, ^{29}Si and ^{30}Si in the TO replica region of the bound exciton (BE) and bound multi-exciton complexes (BMEC) are shown in Fig. 1. The spectra of the natural Si, ^{28}Si and ^{30}Si samples are dominated by the B impurity showing strong B BE (B^1_{TO}) and BMEC transition lines with a weaker P BE (α^1_{TO}) line [27]. The natural Si sample was intentionally lightly doped with 1×10^{15} cm^{-3} B impurities and, using the method introduced by Tajima [28,29], we estimate the impurity concentration in the ^{28}Si sample to be [B] $= 7\times10^{14}$ cm^{-3} and [P] $= 7\times10^{13}$ cm^{-3}, in good agreement with previous Hall measurements [30], and in the ^{30}Si sample approximately [B] $= 2\times10^{15}$ cm^{-3}. The uncertainty in estimating the impurity concentration using the method of Tajima [28,29] is bigger for the ^{30}Si sample due to the weaker TO phonon assisted transition line of the free exciton. The ^{29}Si crystal is dominated by the P impurity showing a strong P BE (α^1_{TO}) transition line (Fig. 1(c)) and the P concentration

Table 1
The isotopic composition and average isotopic mass of the samples investigated

Sample	Isotopic composition	Average mass (amu)
Natural Si	92.23% (^{28}Si) + 4.67%(^{29}Si) + 3.10% (^{30}Si)	28.086
^{28}Si	99.896 % (^{28}Si)	27.978
^{29}Si	97.58% (^{29}Si) + 2.15%(^{28}Si) + 0.27% (^{30}Si)	28.958
^{30}Si	98.68% (^{30}Si) + 0.62%(^{29}Si) + 0.70% (^{28}Si)	29.954
^{28}Si + ^{30}Si	26% (^{28}Si) + 74% (^{30}Si)	29.45

is estimated to be approximately $[P] = 1.5 \times 10^{15}$ cm^{-3}. The BE and BMEC TO replicas are energetically shifted due to the different isotopic composition of the samples. This energy shift is composed of two contributions: the shift of the electronic band gap and the shift of the TO phonon energy. From the no-phonon recombination of the P and B BE we can obtain the energy shift of the band gap. Due to the much simpler electronic structure of the donor P BE, shown in Fig. 2 for all samples, these transitions were used to obtain the band gap shifts. The no-phonon P BE exciton spectrum in silicon consists of only one sharp line, as seen for natural and isotopically pure ^{28}Si in Fig. 2(a) and (b). The broadening and splitting of the no-phonon P BE transition line in Fig. 2(c) and (d) has been shown to result from carbon contamination [31]. Previous studies have indicated that in isotopically enriched ^{28}Si crystals with moderate impurity concentration, the no-phonon BE transitions are much sharper than in natural silicon [4]. From the energy shifts of the indirect electronic band gap

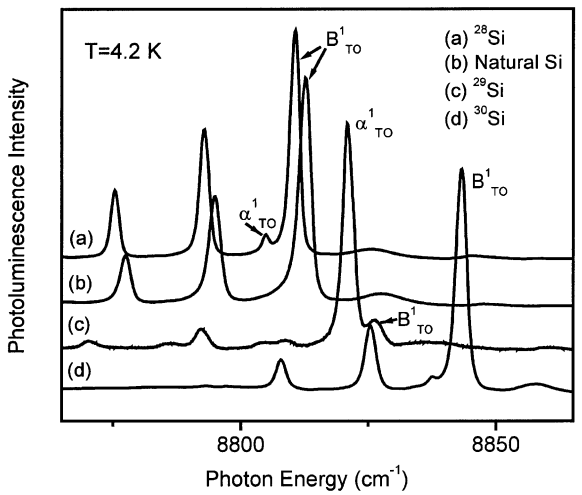

Fig. 1. PL spectra of natural Si; isotopically enriched ^{28}Si, ^{29}Si and ^{30}Si in the TO phonon replica region are superimposed. The natural Si, ^{28}Si and ^{30}Si spectra are dominated by the boron BE (B^1) and BMEC lines, while the ^{29}Si spectrum shows a stronger phosphorus BE (α^1) line. The energetic shift between the spectra is due to the indirect electronic band gap and wave-vector conserving phonon shifts. The spectra were collected using Ar^+ laser excitation, and a spectral resolution of 0.1 cm^{-1}.

relative to the ^{28}Si sample, we were able to estimate the zero-point renormalization energies, using Eq. (4). The four obtained renormalization energies are listed in Table 2; they are similar to the value found for germanium (-51.9 ± 2.1 meV) using the same experimental method [7]. The energy shift of the direct electronic band gap (E_0', E_1) of Si with isotopic composition measured recently using ellipsometry, led to a renormalization energy of -90 meV [32].

We discuss next the phonon frequency shifts induced by the isotopic composition and the different mechanisms that contribute to these shifts. The frequency shifts for the TO and TA wave-vector conserving phonons were obtained from the phonon replicas of the BE transitions. We give all phonon shifts relative to the ^{28}Si sample, because of its high isotopic purity. The phonon energy shifts of natural silicon compared to ^{28}Si have been published elsewhere [4], but are given in Table 3 for completeness. In addition to the phonon shifts theoretically predicted by the VCA, the additional anharmonic contributions to this frequency shift for the Raman phonon have been estimated.

Previous investigations have shown that the Raman phonon has a probability of 95% to decay into combinations of longitudinal and transverse acoustic (LA + TA) phonons [19]. This decay process determines the lifetime of the Raman phonon. The anharmonic contributions to the Raman phonon frequency shift result from phonon interaction processes (for a more detailed analysis see Ref. [2]). These processes can be estimated using perturbation theory and give an additional correction term to the frequency shift predicted by the VCA. This correction term is proportional to the inverse average vibrating mass. In total, the frequency of the Raman phonon is given by

$$\omega(\bar{M}) = \omega_0 \sqrt{\frac{M_{28}}{\bar{M}}} + \Delta_{\text{anh}} \frac{M_{28}}{\bar{M}} \tag{6}$$

where ω_0 is the bare harmonic frequency, $\bar{M}$ the average mass and M_{28} the isotopic mass of ^{28}Si [18]. This frequency is not measurable directly, because the experiment probes only phonons that are renormalized through such phonon–phonon interaction processes, but it can be estimated from the temperature dependence of the Raman shift [18,33,34]. The experimental data of Ref. [33] have been used to estimate the total renormalization of the Raman frequency at $T = 0$ K. With $\Delta_{\text{anh}} = -5.6$ cm^{-1} and the harmonic Raman

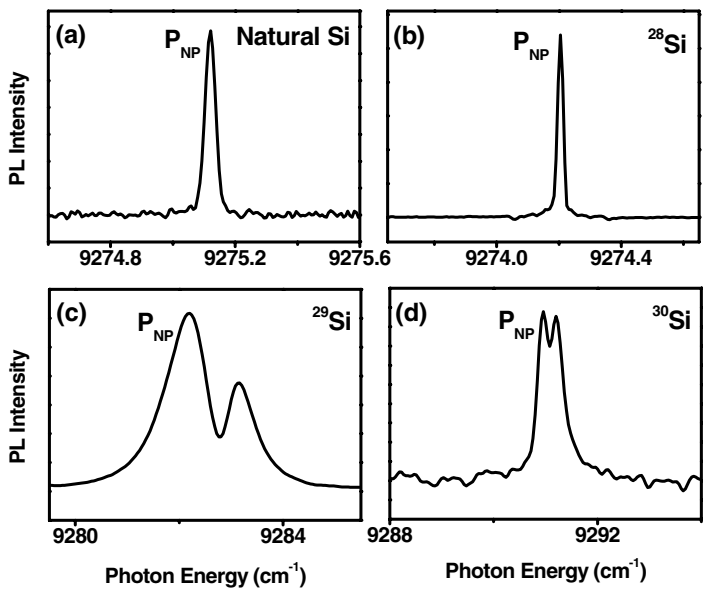

Fig. 2. PL spectra of the phosphorus BE no-phonon transition lines. While in natural Si and ^{28}Si these transition lines are very sharp, in the ^{29}Si and ^{30}Si samples these transitions are split and broadened likely due to carbon contamination. The difference in energy between these transitions is due to the shift of the indirect electronic band gap with isotopic composition. The spectra were collected using 1020 nm Ti/sapphire laser excitation. The spectral resolution applied to the PL spectra of natural Si and ^{28}Si was 0.02 cm^{-1}, and to the PL spectra of ^{29}Si and ^{30}Si, 0.1 cm^{-1}.

frequency in ^{28}Si $\omega_0 = 530.2$ cm^{-1} [18], the expected frequency shift for the Raman phonon in natural Si (0.83 cm^{-1}) is very close to the measured one of (0.81 cm^{-1}).

The CPA also predicts a small disorder-induced frequency shift [18]. In isotopic mixtures, with a much higher isotopic disorder, the disorder induced frequency shift becomes more important for the Raman phonon. The TO and TA phonon shifts listed in Table 3 are also in agreement with the VCA. Small deviations from the VCA are mainly due to the isotopic disorder, caused by the random distribution of the ^{29}Si and ^{30}Si isotopes in natural Si and, by a smaller amount, by anharmonic effects. Due to the much higher one-phonon DOS for the TO and TA wave-vector conserving phonons, the CPA predicts a higher disorder-induced frequency shift than for the Raman phonon [18]. Estimations of the frequency shift using the CPA are very complex and will be included in future publications. In order to estimate the anharmonic effects for the TO and TA phonons, we need to know their bare harmonic frequency in ^{28}Si and the total renormalization of their frequency at $T = 0$ K in natural Si.

The isotopically enriched ^{29}Si sample contains mainly P as electrically active impurity and the broadening and splitting of the P no-phonon line, shown in Fig. 2, may be due to carbon contamination [31]. The broadening and splitting of the P no-phonon line increases the experimental error in determining the band gap and TO phonon shift relative to the ^{28}Si sample. Nevertheless, the TO phonon frequency shift agrees well with the value predicted by the VCA. Possible disorder-induced frequency shift due to the 2.15 % ^{28}Si still contained in the sample is much smaller than our experimental certainty.

In addition, we investigated an isotopically disordered alloy with an isotopic mixture of ^{28}Si and ^{30}Si grown by liquid-phase epitaxy from indium (In) solution. The isotopic

Table 2
The indirect electronic band gap shifts relative to the isotopically enriched ^{28}Si sample. The renormalization energies are obtained from these band gap shifts using eq. (4). The band gap shifts are given in both (cm^{-1}) and (meV) for ease of comparison with previous works

	Natural Si	Enriched ^{29}Si	Enriched ^{30}Si	Mixture of ^{28}Si + ^{30}Si
Band Gap Shift	0.92 cm^{-1} 114 μeV	8.4 cm^{-1} 1.04 meV	16.9 cm^{-1} 2.09 meV	12 cm^{-1} 1.48 meV
Band Gap Renormalization	−59.2 meV (±1 meV)	−60.4 meV (±2 meV)	−61.3 meV (±1 meV)	−57.7 meV (±2 meV)

Table 3
The experimentally obtained energy shifts of the TO, TA and Raman phonons are summarized together with the energetic shifts predicted by the VCA for natural Si compared to isotopically enriched ^{28}Si. For the Raman phonon the anharmonic contributions to the shift have been included

	TO phonon (cm^{-1})	TA phonon (cm^{-1})	Raman phonon (cm^{-1})
Phonon shift of natural Si measured with respect to ^{28}Si	−1.14 (±0.1)	−0.28 (±0.1)	−0.81 (±0.05)
Corresponding shifts predicted from the VCA (harmonic contributions) compared to ^{28}Si	−0.91	−0.29	−1.01
Predicted shifts including anharmonic contributions			−0.83

Table 4
The experimentally obtained energetic shifts of the TO phonons are summarized together with the energetic shifts predicted by the VCA for ^{29}Si and isotopic mixture (^{28}Si + ^{30}Si) compared to isotopically enriched ^{28}Si

	Enriched ^{29}Si (cm^{-1})	Mixture of ^{28}Si and ^{30}Si(cm^{-1})
TO phonon shifts measured with respect to ^{28}Si	−7.8 (±0.5)	−12.6 (±0.5)
Corresponding shifts predicted from the VCA compared to ^{28}Si	−8	−11.9

composition and average atomic mass are given in Table 1. The PL spectrum showed a high concentration of indium and phosphorus that could not be determined exactly but we estimate to be of order 1×10^{16} cm^{-3} or greater, based on the P-In donor–acceptor pair PL [35]. From the no-phonon P BE transition line we were able to determine the band gap shift and from the TO phonon assisted PL transition line, the frequency of the TO phonon. In such highly isotopically disordered materials, the disorder induced phonon frequency shift and linewidth broadening become significant. The discrepancy between the VCA predicted frequency shift and the measured value, given in Table 4, can thus be safely attributed to the isotopic disorder induced shift. In fact, recent calculations using the CPA [18] predict for the TO(X) phonon in a crystal with this isotopic composition a disorder-induced frequency shift of -0.5 cm^{-1}, in good agreement with our experimental value.

We present next our results for the high isotopically enriched ^{30}Si crystal. The isotopic composition determined by mass spectrometry is given in Table 1. The high isotopic purity is reconfirmed through our PL investigations but a small broadening and splitting of the P BE no-phonon transition line indicate some carbon contamination. It has been shown that the linewidth of the TO(X) phonon is significantly influenced by the isotopic disorder [11,18,21,23,24]. The linewidth of the TO(X) phonon assisted (B^3_{TO}) PL transition line of the BMEC transitions in natural Si is reduced by (0.56 ± 0.03) cm^{-1} in the almost single isotope ^{28}Si crystal. The linewidth of the same transition line is only (0.11 ± 0.03) cm^{-1} broader in ^{30}Si compared to the ^{28}Si crystal, indicating very low isotopic disorder. The phonon replica of the BE and BMEC transitions are not optimal to estimate the changes in the phonon lifetime due to the broadening induced by the underlying electronic structure. The errors given are those arising from line fitting only. From the energy shift of the B^1_{TO} and B^1_{TA} emission, the TO and TA phonon assisted transition lines, we determine the frequency shift of the TO and TA phonon. These shifts are listed in Table 5 and are in good agreement with the value predicted by the VCA, inside the experimental uncertainty. This reconfirms the high isotopic purity of the crystal, showing a very weak isotopic disorder induced frequency shift.

In conclusion, we have determined the indirect band gap shifts of natural Si, ^{29}Si, ^{30}Si and an isotopically mixed sample, relative to the almost single isotope ^{28}Si crystal. These shifts are, as expected from Eq. (3), proportional to the inverse square root of the average atomic masses. Using Eq. (4), from the same pairs of crystals we have estimated the zero-point renormalization energies that are in good agreement inside the limits of the experimental certainty. We have measured the phonon frequency shifts relative to isotopically pure ^{28}Si sample and compared them with the values predicted by the VCA. Finally, the eventual

Table 5
The experimentally obtained energetic shifts of the TO and TA phonons are summarized together with the energetic shifts predicted by the VCA for ^{30}Si compared to isotopically enriched ^{28}Si

	TO phonon (cm^{-1})	TA phonon (cm^{-1})
Measured phonon shift of ^{30}Si vs ^{28}Si	−15.7 (±0.2)	−5.1 (±0.2)
Corresponding shifts predicted from the VCA (harmonic contributions)	−15.7	−5.1

discrepancies due to anharmonic and disorder effects have been discussed.

Acknowledgments

This work was supported by the National Science and Engineering Research Council of Canada.

References

[1] M. Cardona, Phys. Stat. Sol. (b) 220 (2000) 5.
[2] M. Cardona, T. Ruf, Solid State Commun. 117 (2001) 201.
[3] E.E. Haller, J. Appl. Phys. 77 (1995) 2857.
[4] D. Karaiskaj, M.L.W. Thewalt, T. Ruf, M. Cardona, H.-J. Pohl, G.G. Deviatych, P.G. Sennikov, H. Riemann, Phys. Rev. Lett. 86 (2001) 6010.
[5] G. Davies, E.C. Lightowlers, K. Itoh, W.L. Hansen, E.E. Haller, V. Ozhogin, Semicond. Sci. Technol. 7 (1992) 1271.
[6] G. Davies, E.C. Lightowlers, T.S. Hui, V. Ozhogin, K.M. Itoh, W.L. Hansen, E.E. Haller, Semicond. Sci. Technol. 8 (1993) 2201.
[7] A.T. Collins, S.C. Lawson, G. Davies, H. Kanda, Phys. Rev. Lett. 65 (1990) 891.
[8] P. Etchegoin, J. Weber, M. Cardona, W.L. Hansen, K. Itoh, E.E. Haller, Solid State Commun. 83 (1992) 843.
[9] S. Zollner, M. Cardona, S. Gopalan, Phys. Rev. B 45 (1992) 3376.
[10] C. Parks, A.K. Ramdas, S. Rodriguez, K.M. Itoh, E.E. Haller, Phys. Rev. B 49 (1994) 14244.
[11] K.C. Hass, M.A. Tamor, T.R. Anthony, W.F. Banholzer, Phys. Rev. B 45 (1992) 7171.
[12] K.C. Hass, M.A. Tamor, T.R. Anthony, W.F. Banholzer, Phys. Rev. B 44 (1991) 12046.
[13] J.M. Zhang, M. Giehler, A. Göbel, T. Ruf, M. Cardona, E.E. Haller, K. Itoh, Phys. Rev. B 57 (1998) 1348.
[14] A. Göbel, D.T. Wang, M. Cardona, L. Pintschovious, W. Reichardt, J. Kulda, N.M. Pyka, K. Itoh, E.E. Haller, Phys. Rev. B 58 (1998) 10510.
[15] P. Lautenschlager, P.B. Allen, M. Cardona, Phys. Rev. B 31 (1985) 2163.
[16] P. Lautenschlager, P.B. Allen, M. Cardona, Phys. Rev. B 33 (1986) 5501.
[17] F. Widulle, T. Ruf, A. Göbel, I. Silier, E. Schönherr, M. Cardona, J. Camacho, A. Cantarero, W. Kriegseis, V.I. Ozhogin, Physica (Amsterdam) 263B–264B (1999) 381.
[18] F. Widulle, T. Ruf, M. Konuma, I. Silier, M. Cardona, W. Kriegseis, V.I. Ozhogin, Solid State Commun. 118 (2001) 1.
[19] A. Debernardi, S. Baroni, E. Molinari, Phys. Rev. Lett. 75 (1995) 1819.
[20] H.D. Fuchs, C.H. Grein, M. Cardona, W.L. Hansen, K. Itoh, E.E. Haller, Solid State Commun. 82 (1992) 225.
[21] P. Etchegoin, H.D. Fuchs, J. Weber, M. Cardona, L. Pintschovius, N. Pyka, K. Itoh, E.E. Haller, Phys. Rev. B 48 (1993) 12661.
[22] H.D. Fuchs, C.H. Grein, M. Bauer, M. Cardona, Phys. Rev. B 45 (1992) 4065.
[23] H.D. Fuchs, C.H. Grein, R.I. Devlen, J. Kuhl, M. Cardona, Phys. Rev. B 44 (1991) 8633.
[24] H.D. Fuchs, C.H. Grein, C. Thomsen, M. Cardona, W.L. Hansen, E.E. Haller, K. Itoh, Phys. Rev. B 43 (1991) 4835.
[25] G. Nelin, G. Nilsson, Phys. Rev. B 5 (1972) 3151.
[26] G. Nilsson, G. Nelin, Phys. Rev. B 6 (1972) 3777.
[27] M.L.W. Thewalt, in: E.I. Rashba, M.D. Sturge (Eds.), Excitons, North-Holland, Amsterdam, 1982, pp. 393–458.
[28] M. Tajima, Appl. Phys. Lett. 32 (1978) 719.
[29] E.C. Lightowler, in: R.A. Stradling, P.C. Klipstein (Eds.), Growth and characterization of semiconductors, Adam Hilger, Bristol, 1990, p. 135.
[30] T. Ruf, R.W. Henn, M. Asen-Palmer, E. Gmelin, M. Cardona, H.-J. Pohl, G.G. Devyatych, P.G. Sennikov, Solid State Commun. 115 (2000) 243.
[31] A.N. Safonov, G. Davies, E.C. Lightowler, Phys. Rev. B 54 (1996) 4409.
[32] L.F. Lastras-Martínez, T. Ruf, M. Konuma, M. Cardona, D.E. Aspnes, Phys. Rev. B 61 (2000) 12946.
[33] E. Haro, M. Balkanski, R.F. Wallis, K.H. Wanser, Phys. Rev. B 34 (1986) 5358.
[34] J. Menéndez, M. Cardona, Phys. Rev. B 29 (1984) 2051.
[35] U.O. Ziemelis, M.L.W. Thewalt, R.R. Parsons, Appl. Phys. Lett. 39 (1981) 972.